1.60-1.57 Ga suprasubduction zone model for metal endowment in eastern Australia

Caroline Tiddy
MinEx CRC
Future Industries Institute
University of South Australia
Mawson Lakes 5095
South Australia
caroline.tiddy@unisa.edu.au

David Giles
MinEx CRC
Future Industries Institute
University of South Australia
Mawson Lakes 5095
South Australia
david.giles@unisa.edu.au

SUMMARY

We propose a model that places development of IOCG (and porphyry-epithermal) mineralisation at ca. 1.60-1.57 Ga in eastern Proterozoic Australia into the context of a modern-day subduction zone. The model is comparable to modern analogues of the Late Cretaceous to Early Eocene Laramide Orogeny in the western United States, present-day slab geometries in the Andes of South America, and by the formation of Cretaceous IOCG and Cu-porphyry deposits in the Chilean Coastal Cordillera.

The model depicts a change from rollback subduction geometry and development of extensional basins in the overriding plate (~1.67 – 1.604 Ga) to flat-slab subduction at 1.604 Ga. The change in subduction architecture was triggered by the arrival of a buoyant oceanic plateau at the subduction site. Slab-melting and metasomatism of the subcontinental lithospheric mantle (SCLM) resulted in eclogitasation and densification of the frontal oceanic slab, slab steepening, sudden upwelling of hot asthenosphere, and production of anhydrous, F-rich, S-poor melts that interacted with the metasomatised SCLM. Resultant mafic melts underwent fractionation and eventually formed the dominantly A-type Hiltaba Suite granites and Gawler Range Volcanics and were associated with IOCG mineralisation. The downgoing slab steepened and retreated, which can be tracked by the progressive westerly to southwesterly younging direction of the Hiltaba Suite. Slab retreat resulted in further asthenospheric upwelling and progressive development of an asthenospheric wedge in a normal subduction geometry. Heat introduced from the asthenospheric wedge resulted in dehydration of buoyant oceanic lithosphere and production of S-rich fluids that interacted with the asthenosphere to produce oxidised, S-rich partial melts. Within this architecture, the spatial and temporal distribution of IOCG and porphyry-epithermal mineral systems in the Gawler Craton is dictated by the evolution of the subducting slab and the chemistry of the fluids/melts derived from the subducting slab.

Key words: Proterozoic Australia, IOCG mineralisation, SCLM metasomatism, Slab retreat, Slab melting, Slab dehydration, Felsic flare-up.

INTRODUCTION

The geological history of eastern Australia from 1.60 to 1.57 Ga is a period of continent-scale deformation and metamorphism, voluminous magmatism and generation of large iron oxide-copper–gold (IOCG) mineralisation including the Olympic Dam deposit (Figure 1). Published tectonic models for this period range from intracratonic (e.g. Wyborn *et al.,* 1987) to suprasubduction zone settings (e.g. Betts and Giles, 2006; Hand *et al.,* 2007; Forbes *et al.,* 2008), with variable importance placed on the significance of spatially and temporally coincident magmatism and its role in ore genesis (e.g. Williams *et al.,* 2005; Groves *et al.,* 2010; Reid, 2019).

We present an alternative tectonic model for eastern Proterozoic Australia from c. 1.67–1.58 Ga as proposed by Tiddy and Giles (2020). The model places Proterozoic Australia in the context of a suprasubduction zone and provides a mechanism for generation of the F-rich, anhydrous 'A-type' magmatism that is associated with IOCG mineralisation in the Gawler Craton and has implications for the formation of IOCG (and porphyry-epithermal) mineralisation. Similarities between this model and the Phanerozoic features of the western United States and the Chilean Coastal Cordillera are discussed.

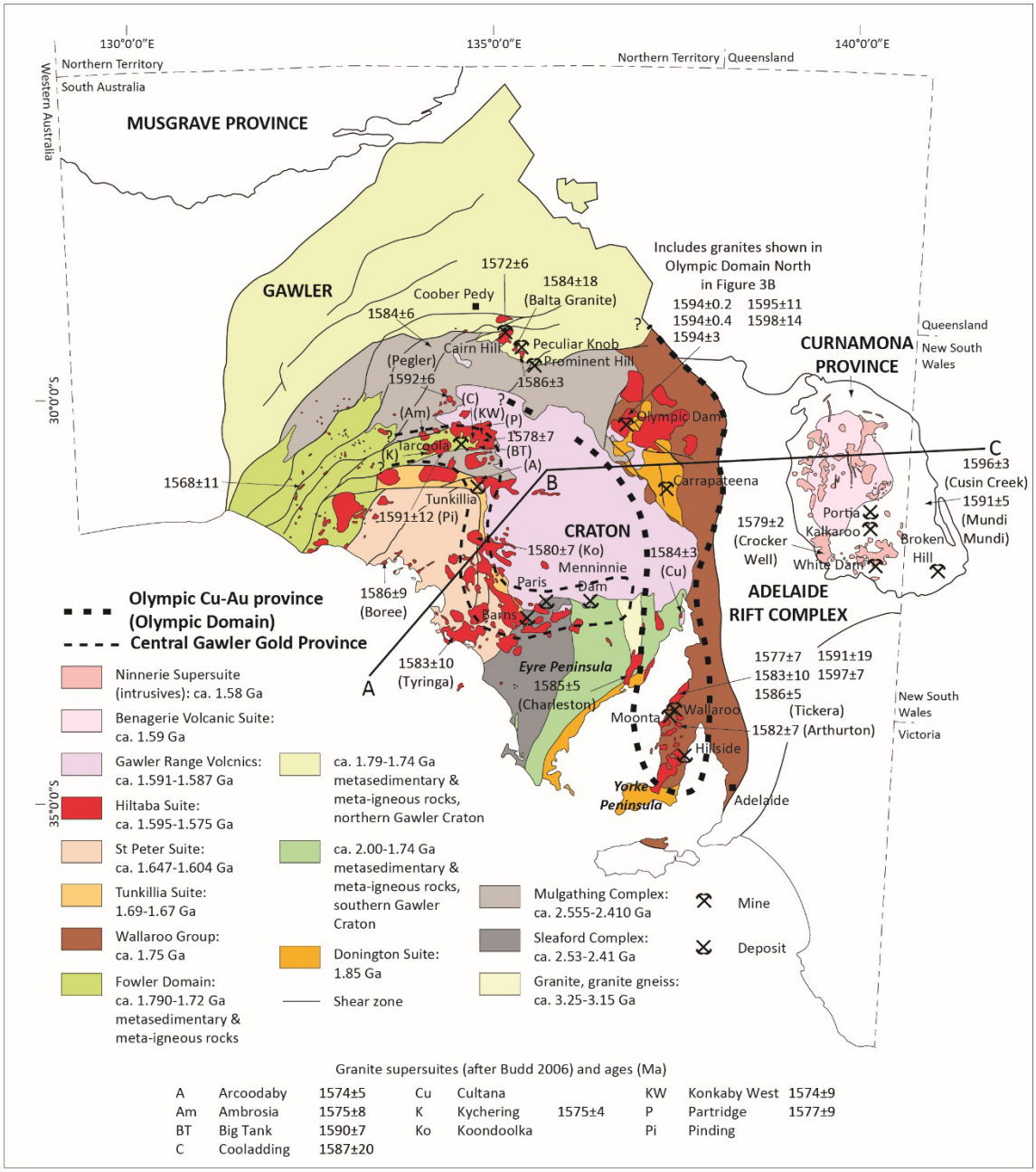

Figure 1. Interpreted solid geology map of the Gawler Craton and Curnamona Province showing the Olympic Domain, Central Gawler Gold Province, major IOCG deposits and U-Pb crystallisation age data for the Hiltaba Suite. Taken from Tiddy and Giles (2020).

c. 1.60-1.57 Ga ACTIVITY IN AUSTRALIA

Tiddy and Giles (2020) describe the geological features of eastern Proterozoic Australia leading into and following the c. 1.60–1.57 Ga time slice in detail. Key geological features that need to be accounted for in a tectonic model for this time period include: switching between intense shortening and extensional tectonic regimes; extensive high-temperature/low-pressure metamorphism and contemporaneous deformation followed by exhumation of terranes in the South Australian Craton; voluminous older A-type to younger I-type magmatism (Hiltaba Suite) in the northern Olympic Domain to the southwestern Gawler Craton at ca. 1.60-1.57 Ga, respectively; extrusion of voluminous, hot (~950–1,100°C), A-type, F-rich lavas of the Gawler Range Volcanics at c. 1.595–1.587 Ga; transition in Nd isotopic values from crustal (e.g., c. 1.74 Ga McGregor Volcanics) to mantle (c. 1.65–1.60 Ga St Peter Suite) compositions/signatures; metasomatism of the subcontinental lithospheric mantle (SCLM) beneath the Gawler Craton; generation of extensive IOCG mineralisation (e.g. Olympic Dam) paired with Au-only (e.g. Tunkillia, Tarcoola) and base metal (e.g. Minninnie Dam, Paris) mineralisation; spatial relationships between mineralisation and magmatism; and, consistency with tectonic settings leading into and following c. 1.60–1.57 Ga.

SUPRASUBDUCTION ZONE MODEL

Two end-member models have been published for the 1.60-1.57 Ga time slice: mantle plume interaction with a subduction zone (Betts *et al.,* 2009); and foundering/delamination of fertile, metasomatised lithospheric mantle in a post-subduction setting (Skirrow *et al.,* 2018). Both models account for several factors required to explain the 1.60–1.57 Ga period; although, as discussed by Tiddy and Giles (2020), have limitations. The alternative model proposed by Tiddy and Giles (2020) (Figure 2) draws on aspects of both models and is summarised below.

c. 1.67–1.604 Ga

From c. 1.67–1.604 Ga, a north-dipping, rollback subduction zone is interpreted at the southern margin of the Gawler Craton. The evolution of this subduction zone is evidenced by a shift towards positive εNd values of felsic magmatic rocks in the central and southwest Gawler Craton between 1.74 and 1.60 Ga (see also figure 7 in Tiddy and Giles, 2020), and the calc-alkaline nature and juvenile isotopic composition of the c. 1.65–1.604 Ga St Peter Suite (Symington *et al.,* 2014; Reid *et al.,* 2019). Rollback of the subduction zone resulted in extension and lithospheric thinning in the overriding plate, development of back-arc basins and elevated crustal thermal gradients (e.g., Forbes *et al.,* 2008; Raveggi *et al.,* 2007; Figure 2).

c. 1.604–1.595 Ga

Arrival of a buoyant oceanic plateau at the subduction trench at c. 1.604 Ga triggered a switch from rollback to flat-slab subduction at c. 1.604–1.595 (Figure 2a–c), terminating arc magmatism of the St Peters Suite and producing small volume intrusive magmas manifest as the oldest phases of the Hiltaba Suite. Compressive stresses were transferred into the continental interior resulting in periods of intense shortening focused within earlier developed, thermally weakened back-arc basins (e.g., Olarian Orogeny, Forbes *et al.,* 2008) and around the rigid Archean nucleus of the Gawler Craton (e.g., c. 1.60–1.58 Ga deformation in the Coober Pedy Ridge, Mable Creek Ridge, Mount Woods Inlier and Barossa Complex; Hand *et al.,* 2007; Forbes *et al.,* 2012; Morrissey *et al.,* 2013) (Figure 2c).

c. 1.595–1.585 Ga

Differential sinking of the dense frontal section of typical oceanic lithosphere that was attached to the buoyant posterior oceanic plateau ultimately led to slab tearing (and potentially complete decoupling) and asthenospheric upwelling at the leading edge of the buoyant slab (Figure 2c-d). Maximum differential stresses were focussed beneath the present-day Olympic Dam area. Asthenospheric upwelling resulted in elevated temperatures, F-enrichment and partial melting of the SCLM, and production of F-rich mafic melts now recognised within the Hiltaba Suite (e.g., Wade *et al.,* 2019) (Figure 2d). Ascending F-rich SCLM-derived mafic magmas triggered production of large volumes of increasingly siliceous melts that migrated to mid- to upper-crustal magma chambers (Figure 2d) and evolved into highly fractionated melts enriched in incompatible elements (e.g., F, Cl, REE, U; Stewart and Foden, 2003; Agangi *et al.,* 2010, 2012). These melts are today recognised as the as the anhydrous, F-rich, A-type magmas of the Hiltaba Suite and Gawler Range Volcanics (Roxby Downs Granite) and the mafic to felsic lavas of the c. 1.595–1.589 Ga lower Gawler Range Volcanics (Jagodzinski *et al.,* 2016; McPhie *et al.,* 2020; Figure 2d). In the Olympic Dam area, Hiltaba Suite granites were shallowly emplaced and then rapidly exhumed during transient lithospheric thinning (Figure 2d) and overprinted by IOCG mineralisation at c. 1.594–1.590 Ga (Cherry *et al.,* 2018; Courtney-Davies *et al.,* 2019; McPhie *et al.,* 2020).

c. 1.585–1.575 Ga

After c. 1.59 Ga, progressive eclogitisation and densification of the flat slab resulted in failure of flat-slab subduction, propagation of hot asthenosphere into a newly created mangle wedge, migration Hiltaba Suite magmatism towards the central and southwest Gawler Craton and a change from A-type to I-type granite compositions (Figure 2e). The younger I-type components of the Hiltaba Suite were generated from partial melting of relatively juvenile, hydrated and S-rich lithosphere at the location of earlier c. 1.65–1.605 Ga arc magmatism (Figure 2e). Magmatism was accompanied by mineralisation in the Mt Woods Inlier (c. 1.585 Ga; Belperio *et al.,* 2007), Yorke Peninsula (1.585 Ga; Gregory *et al.,* 2011) and the Central Gawler Gold Province (c. 1.58 Ga; Budd and Fraser, 2004; Nicolson *et al.,* 2017).

Post c. 1.575 Ga

The youngest Hiltaba Suite plutons were emplaced at c. 1.575 Ga and mark the end of flat-slab subduction and the shift of convergent margin activity away from the Gawler Craton. Cessation of flat-slab subduction may have been caused by eclogitisation, steepening and eventual detachment of the entire flat slab section (see also figure 12 in Skirrow *et al.,* 2018); decoupling of the dense frontal slab from the buoyant oceanic plateau, which rebounded and accreted to the base of the lithosphere (Figure 2e, f); or the dense apron of normal oceanic lithosphere was removed and subducted, and the buoyant oceanic plateau accreted to the base of the lithosphere.

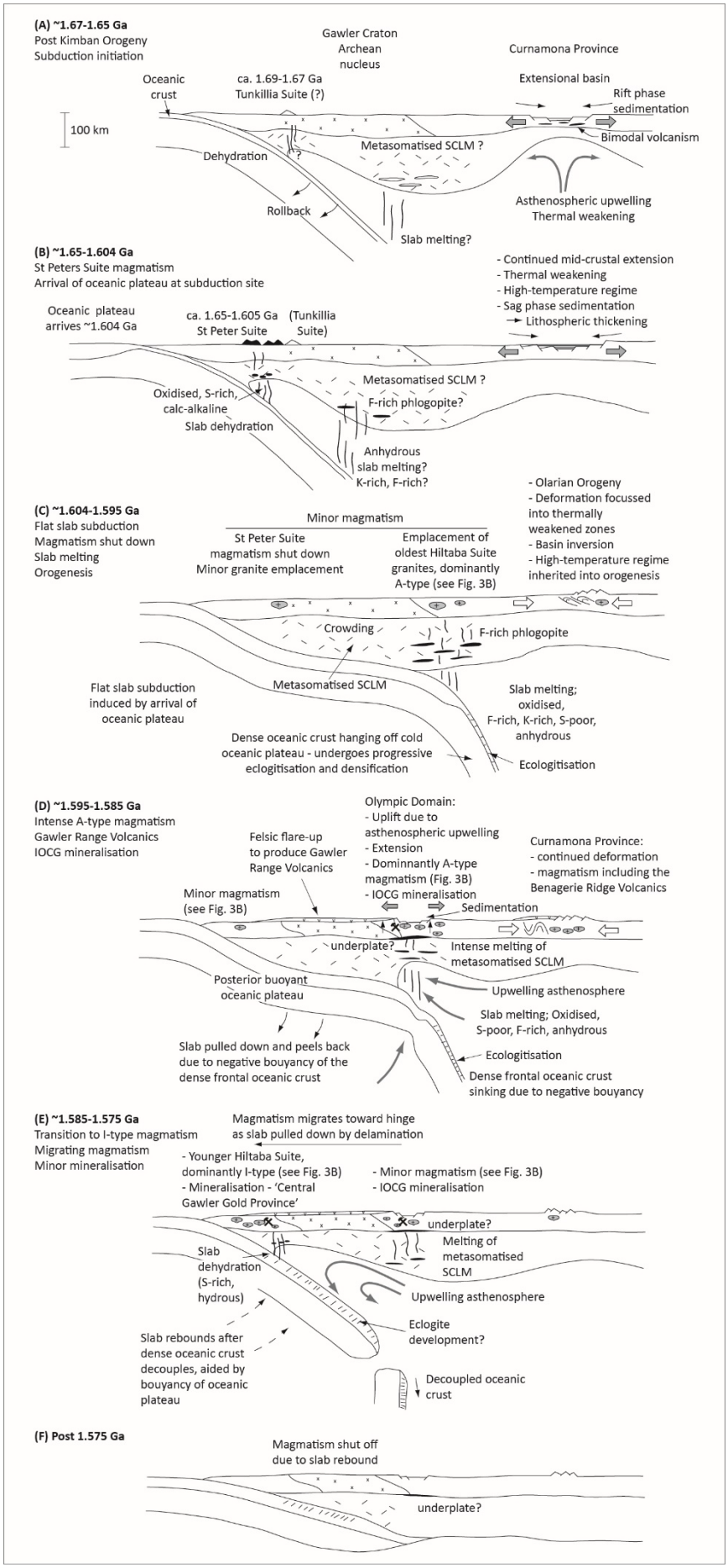

Figure 2. Alternative model for the 1.60-1.57 Ga evolution of eastern Proterozoic Australia. Taken from Tiddy and Giles (2020).

PHANEROZOIC COMPARISONS

The model presented here has similarities with the c. 80-50 Ma Laramide Orogeny in the western United States (e.g., Liu and Currie 2016 and references therein) including:

- flat-slab subduction triggered by variations in plate motion combined with subduction of a thick, buoyant oceanic plateau subduction, and associated with transfer of compressional stresses inboard of the plate margin, progressive deformation, exhumation/uplift and the shut-down of a pre-existing magmatic arc.
- a subsequent change to a rollback subduction geometry and retreat of the downgoing slab resulting in eclogitisation, densification and subsequent removal of the previously buoyant oceanic plateau, asthenospheric upwelling, magmatism associated with lithospheric extension and formation of metamorphic core complexes.

Similarities between this model and convergent margin IOCG terranes such as the Cretaceous Coastal Cordillera of Chile between 21° and 30°S (Sillitoe, 2003; Chen *et al.,* 2013) include:

- IOCG mineralisation developing during transient periods of extension within the convergent margin.
- spatiotemporal associations between mineralisation and voluminous magmatism.
- ore fluids being derived from devolatisation of mantle-derived magmas and transported along regional-scale pathways.
- ore deposits being structurally controlled and host within a range of lithology types and ages.
- tectonic setting of slab rollback and extension switching to compression, magmatism and mineralisation.

IMPLICATIONS FOR Cu-Au MINERALISATION

Tiddy and Giles (2020) draw on knowledge of modern Cretaceous Andean IOCG systems to inform three key features required to generate ancient IOCG deposits:

1. Generation and preservation of metasomatised/melt-modified SCLM beneath the future site of mineralisation from which elevated high field strength, light rare earth elements, halogens and potentially Cu and Au may be sourced (e.g., Skirrow *et al.,* 2007; Groves *et al.,* 2010).
2. A trigger to induce partial melting of the SCLM (e.g., Begg *et al.,* 2012; Griffin *et al.,* 2013).
3. A lithospheric-scale plumbing system along which melts and fluids can be transported from depth

Tectonic setting of SCLM metasomatism

Regional SCLM metasomatism within suprasubduction zone settings such as that proposed for eastern Proterozoic Australia may be caused by processes including interaction with fluids or melts exposed from the down-going slab (e.g., Köhler *et al.,* 2009), or by interaction with metasomatic fluids derived from a mantle plume independent of subduction processes (e.g. Howarth *et al.,* 2014). Metasomatised SCLM has been shown to be preserved beneath the present-day Archean nucleus of the Gawler Craton and the Olympic Domain (Thiel and Heinson, 2013; Skirrow *et al.,* 2018). However, the absolute timing of SCLM metasomatism is unknown due to the complex and protracted geological history and conjecture in the tectonic setting of the Gawler Craton (e.g., Betts and Giles, 2006; Wade *et al.,* 2006; Payne *et al.,* 2009).

Metasomatism of the SCLM beneath the Gawler Craton may have been associated with mantle plume activity at c. 2.52–2.00 Ga (Wade *et al.,* 2019) and/or with subduction-related settings at c. 2.46–2.41 Ga (Sleafordian Orogeny; Reid *et al.,* 2014) and/or 1.73–1.69 Ga (Kimban Orogeny; e.g. Hand *et al.,* 2007). During the Kimban Orogeny, which is the temporally closes major tectonic event to the c. 1.60–1.57 Ga event, the Archean nucleus of the Gawler Craton is inferred to have been accreted to the North Australian Craton along a north-dipping subduction zone (Betts *et al.,* 2016 and references therein). However, regional subduction-induced metasomatism of the SCLM beneath the Gawler Craton would not have been possible in this geometry because the Gawler Craton was located on the down-going plate rather than in a suprasubduction setting.

Regional subduction-induced metasomatism of the Gawler Craton SCLM in a suprasubduction setting is instead interpreted by Tiddy and Giles (2020) to have occurred leading into the period of flat-slab subduction at c. 1.604-1.595 Ga within the setting of a north-dipping subduction zone initiated to the west of the Gawler Craton and following accretion during the Kimban Orogeny (Figure 2a). This tectonic setting is analogous to the Laramide Orogeny where dehydration of the Farallon flat slab metasomatised the SCLM beneath western North America ~1,000 km inboard from the subduction margin (e.g., Lee, 2005).

Mechanism of SCLM metasomatism

Tiddy and Giles (2020) suggest that the geometry of the subducting slab beneath the Gawler Craton dictated whether the slab underwent dehydration or melting, which controlled F enrichment and therefore influenced composition of SCLM metasomatism at various distances inboard from the subduction margin. During normal subduction, slab dehydration of the downgoing oceanic crust will release oxidised, sulfate-rich fluids during breakdown of hydrous

phases (typically at slab depths of ~100–120 km) and result in an oxidised S-rich mantle wedge (Zellmer *et al.,* 2015; Pons *et al.,* 2016). Fluorine will be retained in the slab and transported to greater depths within F-bearing mica and amphibole end members (Straub and Layne, 2003; Kendrick *et al.,* 2014). Conversely, F will be released and partition into melt phases during slab melting (e.g. Köhler *et al.,* 2009; Straub and Layne, 2003). Significant slab melting can occur when the downgoing slab is stalled in the subduction zone, during flat slab subduction or in failed flat slab subduction where slab rollback causes the slab to steepen into a more normal subduction angle (Mungall, 2002). Tiddy and Giles (2020) suggest a combination of these processes contributed to significant slab melting of the down-going slab in the subduction zone of eastern Proterozoic Australia possibly from as early as c. 1.67 Ga and through to the period of flat-slab subduction and subsequent failure of the flat slab at c. 1.595–1.585 Ga (Figure 2). Consequently, the slab would have become dehydrated and S-depleted beneath the magmatic arc, resulting in SCLM metasomatism beneath the present-day Olympic Dam occurring via interaction with anhydrous, S-poor and F-rich slab melts.

The metasomatised SCLM composition subsequently dictated the style of magmatism and mineralisation in the Gawler Craton between 1.60 to 1.57 Ga so that S-poor, F-rich IOCG deposits and A-type magmatism are preserved in the Olympic Domain as reflected by the F-rich nature of the Gawler Range Volcanics and Hiltaba Suite and S-poor IOCG mineral systems. Conversely, gold-only epithermal deposits and I-type magmatism are preserved in the central Gawler Craton (Central Gawler Gold Province).

Mantle controls on mineralisation style

The composition of the SCLM will dictate the composition of partial melts derived from a metasomatised SCLM, and therefore properties of hydrothermal fluids exsolved from those partial melts (e.g. oxidation state, volatile and complexing agent content and metal carrying capacity; Richards *et al.,* 2017). The S content of mantle-derived partial melts can influence the distribution of Cu porphyry and IOCG deposits in the same tectonic setting, for example Mesozoic IOCG and Cu porphyry deposits in the Chilean Coastal Cordillera (Richards *et al.,* 2017). In general, Cu porphyry mineralisation is associated with oxidised, hydrous, S-rich, calc-alkaline magmas produced from the partial melting of a metasomatised asthenospheric wedge proximal to the subduction zone margin, whereas IOCG mineralisation is associated with S-poor, relatively primitive, oxidised asthenospheric magmas that develop distal from the subduction zone margin (e.g. within a back-arc extensional environment).

Based on the model of Richards *et al.* (2017), Tiddy and Giles (2020) suggest the spatial and temporal relationships between IOCG and porphyry-epithermal mineral systems in the Gawler Craton are linked to the evolution of the subducting slab beneath the Gawler Craton and the chemistry of the fluids/melts derived from the subducting slab. The distribution of these mineral systems as well as the broad tectonic setting including evolving continental margins with transient periods of extension also show similarities to those seen for Mesozoic IOCG and Cu-porphyry deposits in the Andes.

CONCLUSIONS

An alternative suprasubduction model for eastern Proterozoic Australia at c. 1.60-1.57 Ga at a time of IOCG (and porphyry-epithermal) mineralisation has been proposed by Tiddy and Giles (2020). This new model draws on modern-day analogues of the Late Cretaceous to Early Eocene Laramide Orogeny in western North America, present-day slab geometries of the South American Andes and formation of Cretaceous IOCG and Cu-porphyry deposits in the Chilean Coastal Cordillera. Cu–Au mineralisation in the Gawler Craton is linked to mechanisms by which metasomatised SCLM and partial melts favourable for Cu–Au mineralisation can be generated, such that ‘it is not the type of magmatism that was important to the generation of IOCG versus porphyry-epithermal deposits, but rather the type of partial melt produced in the mantle – oxidised, S-poor (IOCG) or S-rich (porphyry-epithermal) and could carry metals – that interacted with the metasomatised SCLM’ (Tiddy and Giles, 2020).

ACKNOWLEDGMENTS

This work has benefited from discussions and reviews from many people, including Bill Collins, Anthony Reid, Graham Begg, Karl Karlstrom, Mark Pawley, John Foden and Claire Wade. This work has been supported by the Mineral Exploration Cooperative Research Centre whose activities are funded by the Australian Government's Cooperative Research Centre Program.

REFERENCES

Agangi, A., Kamenetsky, V.S., and McPhie, J., 2010, The role of fluorine in the concentration and transport of lithophile trace elements in felsic magmas: insights from the Gawler Range Volcanics, South Australia: Chemical Geology, 273, 314–325.

Agangi A., Kamenetsky, V.S., and McPhie, J., 2012, Evolution and emplacement of high fluorine rhyolites in the Mesoproterozoic Gawler Silicic Large Igneous Province, South Australia: Precambrian Research, 208–211, 124–144.

Begg, G.C., Griffin,W.L., O'Reilly, S.Y., and Natapov, L.M., 2012, The lithosphere, geodynamics and Archean mineral systems: 34th International Geological Congress, Brisbane, Australia, 2012, Abstracts, p 1870.

Belperio, A., Flint, R., and Freeman, H., 2007, Prominent Hill: a hematite-dominated, iron oxide copper-gold system: Economic Geology, 102, 1499–1510.

Betts, P.G., and Giles, D., 2006, The 1800-1100 Ma tectonic evolution of Australia: Precambrian Research, 144, 92–125.

Betts, P.G., Giles, D., Foden, J., Schaefer, B.F., Mark, G., Pankhurst, M.J., Forbes, C.J., Williams, H.A., Chalmers, N.C., and Hills, Q.G., 2009, Mesoproterozoic plume-modified orogenesis in eastern Precambrian Australia: Tectonics, 28, TC3006.

Betts, P.G., Armit, R.J., Stewart, J., Aitken, A.R.A., Aillères, L., Donchak, P., Hutton, L., Withnall, I., and Giles, D., 2016, Australia and Nuna. In Li, Z.X., Evans, D.A.D., and Murphy, J.B. eds, Supercontinent cycles through earth history: Geological Society Special Publication 424. Geological Society of London, pp 47–81.

Budd, A.R., and Fraser, G.L., 2004, Geological relationships and $^{40}Ar/^{39}Ar$ age constraints on gold mineralisation at Tarcoola, central Gawler gold province, South Australia: Australian Journal of Earth Sciences, 51, 685–699.

Chen, H., Cooke, D.R., and Baker, M.J., 2013, Mesozoic iron oxide copper-gold mineralization in the Central Andes and the Gondwana supercontinent breakup, Economic Geology, 108, 37–44.

Cherry, A.R., Ehrig, K., Kamenetsky, V.S., McPhie, J., Crowley, J.L., and Kamenetsky, M.B., 2018, Precise geochronological constraints on the origin, setting and incorporation of c. 1.59 Ga surficial facies into the Olympic Dam Breccia Complex, South Australia: Precambrian Research, 315, 162–178.

Courtney-Davies, L., Tapster, S.R., Ciobanu, C.L., Cook, N.J., Verdugo-Ihl, M.R., Ehrig, K.J., Kennedy, A.K., Gilbert, S.E., Condon, D.J., and Wade, B.J., 2019, A multi-technique evaluation of hydrothermal hematite U-Pb isotope systematics: implications for ore deposit geochronology: Chemical Geology, 513, 54–72.

Forbes, C.J., Betts, P.G., Giles, D., and Weinberg, R., 2008, Reinterpretation of the tectonic context of high-temperature metamorphism in the Broken Hill Block, NSW, and implications on the Palaeo- to Meso-Proterozoic evolution: Precambrian Research, 166, 338–349.

Forbes, C.J., Giles, D., Jourdan, F., Sato, K., Omori, S., and Bunch, M., 2012, Cooling and exhumation history of the northeastern Gawler Craton, South Australia: Precambrian Research, 200–203, 209–238.

Gregory, C., Reid, A., Say, P., and Teale, G., 2011, Project PGC01-06: U-Pb geochronology of hydrothermal allanite and titanite and magmatic zircon from the Hillside Cu-Au deposit, Yorke Peninsula. In Reid, A.J., and Jagodzinski, E.A., Eds, PACE Geochronology: Results of collaborative geochronology projects 2009-10: Report Book 2011/00003, Department of Primary Industries and Resources South Australia, pp 95–126.

Griffin, W.L., Begg, G.C., and O'Reilly, S.Y., 2013, Continental-root control on the genesis of magmatic ore deposits, Nature Geoscience, 6, 905–910.

Groves, D.I., Bierlein, F.P., Meinert, L.D., and Hitzman, M.W., 2010, Iron oxide copper-gold (IOCG) deposits through earth.history: implications for origin, lithospheric setting, and distinction from other epigenetic iron oxide deposits: Economic Geology, 105, 641–654.

Hand, M., Reid, A., and Jagodzinski, L., 2007, Tectonic framework and evolution of the Gawler Craton, South Australia: Economic Geology, 102, 1377–1395.

Howarth, G.H., Barry, P.H., Pernet-Fisher, J.F., Baziotis, I.P., Pokhilenko, N., Pokhilenko, L.N., Bodnar, R.J., Taylor, L.A., and Agashev, A.M., 2014, Superplume metasomatism: evidence from Siberian mantle xenoliths: Lithos, 184–187, 209–224.

Jagodzinski, E.A., Reid, A., Crowley, J., McAvaney, S., and Wade, C., 2016, Precise zircon U-Pb dating of a Mesoproterozoic silicic large igneous province: the Gawler Range Volcanics and Benagerie Volcanic Suite, South Australia: Australian Earth Sciences Convention, 26-30 June 2016, Adelaide.

Kendrick, M.A., Jackson, M.G., Kent, A.J.R., Hauri, E.H., Wallace, P.J., and Woodhead, J., 2014, Contrasting behaviours of CO_2, S, H_2O and halogens (F, Cl, Br, and I) in enriched-mantle melts from Pitcairn and Society seamounts: Chemical Geology, 370, 69–81.

Köhler, J., Schönenberger, J., Upton, B., and Mark, G., 2009, Halogen and trace-element chemistry in the Gardar Province, South Greenland: subduction-related mantle metasomatism and fluid exsolution from alkalic melts: Lithos, 113, 731–747.

Lee, C.-T.A., 2005, Trace element evidence for hydrous metasomatism at the base of the North American lithosphere and possible association with Laramide lowangle subduction: The Journal of Geology, 113, 673–685.

Liu, S., and Currie, C.A., 2016, Farallon plate dynamics prior to the Laramide Orogeny: numerical models of flat subduction: Tectonophysics, 666, 33–47.

McPhie, J., Ehrig, K.J., Kamenetsky, M.B., Crowley, J.L., and Kamenetsky, V.S., 2020, Geology of the Acropolis prospect, South Australia, constrained by high-precision CA-TIMS ages: Australian Journal of Earth Sciences, 67, 699–716.

Morrissey, L.J., Hand, M., Wade, B.P., and Szpunar, M., 2013, Early Mesoproterozoic metamorphism in the Barossa Complex, South Australia: links with the eastern margin of Proterozoic Australia: Australian Journal of Earth Sciences, 60, 769–795.

Mungall, J.E., 2002, Roasting the mantle: slab melting and the genesis of major Au and Au-rich Cu deposits: Geology, 30, 915–918.

Nicolson, B., Reid, A., McAvaney, S., Keeling, J., Fraser, G., and Vasconcelos, P., 2017, A Mesoproterozoic advanced argillic alteration system: $^{40}Ar/^{39}Ar$ thermochronology from Nankivel Hill, Gawler Craton: Report Book 2017/00011, Department of the Premier and Cabinet, South Australia, Adelaide.

Payne, J.L., Hand, M., Barovich, K.M., Reid, A., and Evans, D.A.D., 2009, Correlations and reconstruction models for the.2500-1500 Ma evolution of the Mawson Continent. In Reddy, S.M., Mazumder, R., Evans, D.A.D., and Collins, A.S., Eds, Palaeoproterozoic supercontinents and global evolution: Geological Society Special Publication, 323, pp 319–355.

Pons, M.-L., Debret, B., Bouilhol, P., Delacour, A., and Williams, H., 2016, Zinc isotope evidence for sulfate-rich fluid transfer across subduction zones: Nature Communications, 7, 13794.

Raveggi, M., Giles, D., Foden, J., and Raetz, M., 2007, High Fe-Ti mafic magmatism and tectonic setting of the Palaeoproterozoic Broken Hill Block, NSW, Australia: Precambrian Research, 156, 55–84.

Reid, A.J., Jagodzinski, E.A., Fraser, G.L., and Pawley, M.J., 2014, SHRIMP U–Pb zircon age constraints on the tectonics of the Neoarchean to early Paleoproterozoic transition within the Mulgathing Complex, Gawler Craton, South Australia: Precambrian Research, 250, 27–49.

Reid, A.J., 2019, The Olympic Cu-Au Province, Gawler Craton: a review of the lithospheric architecture, geodynamic setting, alteration systems, cover successions and prospectivity: Minerals, 9, 371.

Reid, A.J., Pawley, M.J., Wade, C., Jagodzinski, E.A., Dutch, R.A., and Armstrong, R., 2019, Resolving tectonic settings of ancient magmatic suites using structural, geochemical and isotopic constraints: the example of the St Peter Suite, southern Australia: Australian Journal of Earth Sciences, 67, 31–58.

Richards, J.P., Lopez, G.P., Zhu, J.-J., Creaser, R.A., Locock, A.J., and Hamid Mumin, A., 2017, Contrasting tectonic settings and sulfur contents of magmas associated with Cretaceous porphyry Cu±Mo±Au and intrusion-related iron oxide Cu-Au deposits in northern Chile: Economic Geology, 112, 295–318.

Sillitoe, R.H., 2003, Iron oxide-copper-gold deposits: an Andean view: Mineralium Deposita, 38, 787–812.

Skirrow, R.G., Bastrakov, E.N., Barovich, K., Fraser, G.L., Creaser, R.A., Fanning, C.M., Raymond, O.L., and Davidson, G.J., 2007, Timing of iron oxide Cu-Au-(U) hydrothermal activity and Nd isotope constraints on metal sources in the Gawler Craton, South Australia: Economic Geology, 102, 1441–1470.

Skirrow, R.G., van der Weilen, S.E., Champion, D.C., Czarnota, K., and Thiel, S., 2018, Lithospheric architecture and mantle metasomatism linked to iron oxide Cu-Au ore formation: multidisciplinary evidence from the Olympic Dam region, South Australia: Geochemistry, Geophysics, Geosystems, 19, 2673–2705.

Stewart, K., and Foden, J., 2003, Mesoproterozoic granites of South Australia: Report Book 2003/00015, Department of Primary Industries and Resources South Australia, Adelaide.

Straub, S.M., and Layne, G.D., 2003, The systematics of chlorine, fluorine, and water in Izu arc front volcanic rocks: implications for volatile recycling in subduction zones: Geochimica et Cosmochimica Acta, 67, 4179–4203.

Swain, G., Barovich, K., Hand, M., Ferris, G., and Schwarz, M., 2008, Petrogenesis of the St Peter Suite, southern Australia: arc magmatism and Proterozoic crustal growth of the South Australian Craton: Precambrian Research, 166, 283–296.

Symington, N.J., Weinberg, R.F., Hasalová, P., Wolfram, L.C., Raveggi, M., and Armstrong, R.A., 2014, Multiple intrusions and remelting-remobilization events in a magmatic arc: the St.Peter Suite, South Australia: Geological Society of America Bulletin, 126, 1200–1218.

Thiel, S., and Heinson, G., 2013, Electrical conductors in Archean mantle – result of plume interaction?: Geophysical Research Letters, 40, 2947–2952.

Tiddy, C.J., and Giles, D., 2020, Suprasubduction zone model for metal endowment at 1.60-1.57 Ga in eastern Australia: Ore Geology Reviews, 122, 103483.

Wade, B.P., Barovich, K.M., Hand, M., Scrimgeour, I.R., and Close, D.F., 2006, Evidence for early Mesoproterozoic arc magmatism in the Musgrave Block, central Australia: implications for Proterozoic crustal growth and tectonic reconstructions of Australia: Journal of Geology, 114, 43–63.

Wade, C.E., Payne, J.L., Barovich, K.M., and Reid, A.J., 2019, Heterogeneity of the sub-continental lithospheric mantle and 'non-juvenile' mantle additions to a Proterozoic silicic large igneous province: Lithos, 340–341, 87–107.

Williams, P.J., Barton, M.D., Jonson, D.A., Fontboté, L., de Haller, A., Mark, G., Oliver, N.H.S., and Marschik, R., 2005, Iron oxide copper-gold deposits: geology, space-time distribution, and possible modes of origin: Economic Geology, 100, 371–405.

Wyborn, L.A.I., Page, R.W., and Parker, A.J., 1987, Geochemical and geochronological signatures in Australian Proterozoic igneous rocks. In Pharaoh TC, Bechinsale RD and Rickard D eds, Geochemistry and mineralisation of Proterozoic volcanic suites: Geological Society Special Publication, 33, 377–394.

Zellmer, G.F., Edmonds, M., and Straub, S.M., 2015, Volatiles in subduction zone magmatism. In Zellmer GF, Edmonds M and Straub SM eds, The role of volatiles in the genesis, evolution and eruption of arc magmas: Geological Society Special Publication, 410, 1–17.